Monthly Notices of the ROYAL ASTRONOMICAL SOCIETY LETTERS

Mon. Not. R. Astron. Soc. **400,** L1–L5 (2009) doi:10.1111/j.1745-3933.2009.00747.x

GRB090111: extra soft steep-decay emission and peculiar rebrightening

R. Margutti,[1,2⋆] T. Sakamoto,[3] G. Chincarini,[1,2] C. Guidorzi,[4,2] J. Mao,[2,5] F. Pasotti,[2] D. Burrows,[6] P. D'Avanzo,[1] S. Campana,[2] S. D. Barthelmy[3] and N. Gehrels[3]

[1]*Università degli studi Milano Bicocca, P.za della Scienza 3, Milano 20126, Italy*
[2]*INAF Osservatorio Astronomico di Brera, via Bianchi 46, Merate 23807, Italy*
[3]*NASA/Goddard Space Flight Center, Greenbelt, MD 20771, USA*
[4]*Dipartimento di Fisica, Università di Ferrara, via Saragat 1, I-44100, Ferrara, Italy*
[5]*Yunnan Observatory, Chinese Academy of Sciences, Kunming, Yunnan Province, China*
[6]*Department of Astronomy and Astrophysics, Pennsylvania State University, 525 Davey Lab, University Park, PA 16802, USA*

Accepted 2009 August 25. Received 2009 August 21; in original form 2009 June 5

ABSTRACT

We present a detailed study of GRB 090111, focusing on its extra soft power-law photon index $\Gamma > 5$ at the very steep-decay phase emission (power-law index $\alpha = 5.1$, steeper than 96 per cent of gamma-ray bursts detected by *Swift*) and the following peculiar X-ray rebrightening. Our spectral analysis supports the hypothesis of a comoving band spectrum with the peak of the νF_ν spectrum evolving with time to lower values: a period of higher temporal variability in the 1–2 keV light curve ends when the $E_{\rm peak}$ evolves outside the energy band. The X-ray rebrightening shows extreme temporal properties when compared to a homogeneous sample of 82 early flares detected by *Swift*. While an internal origin cannot be excluded, we show these properties to be consistent with the energy injection in refreshed shocks produced by slow shells colliding with the fastest ones from behind, well after the internal shocks that are believed to give rise to the prompt emission have ceased.

Key words: radiation mechanisms: non-thermal – gamma-rays: bursts – X-rays: individual: GRB090111.

1 INTRODUCTION

The unprecedented fast repointing capability of *Swift* (Gehrels et al. 2004) has ushered in a new era in the study of gamma-ray bursts (GRB) sources. A canonical picture of the X-ray afterglow light curve emerged (see e.g. Nousek et al. 2006), with five different components describing the overall structure observed in the majority of events: an initial steep decay, a shallow-decay plateau phase, a normal decay, a jet-like decay component and randomly occurring flares.

The steep-decay phase smoothly connects to the prompt emission (e.g. Tagliaferri et al. 2005), with a typical temporal power-law decay index between 2 and 4 (Evans et al. 2009a): this strongly suggests a common physical origin. The observed spectral softening with time challenges the simplest version of the most popular theoretical model for this phase, the high-latitude emission model (Fenimore, Madras & Nayakshin 1996; Kumar & Panaitescu 2000): according to this scenario, steep-decay photons originate from the delayed prompt emission from different viewing latitudes of the emitting area (Zhang, Liang & Zhang 2007) and are expected to lie on a simple power law (SPL) spectral model. The 0.3–10 keV spectrum of the steep-decay phase is generally consistent with the expected SPL behaviour with a typical photon index $\Gamma \sim 2$ (see Evans et al. 2009a); however, a careful inspection of the GRBs with the best statistics reveals that alternative explanations are required (see e.g. Qin et al. 2009; Zhang et al. 2009). Deviations from the SPL spectral model are, therefore, of particular interest.

Flares have been found to be a common feature of early X-ray afterglows: with a typical duration over occurrence time $\Delta t/t \sim 0.1$ (Chincarini et al. 2007) and a band spectrum (Band et al. 1993) reminiscent of the typical spectral shape of the prompt emission (Falcone et al. 2007), they are currently believed to be related to the late-time activity by the central engine. In spite of the growing statistics, their origin is still an open issue.

In this paper, we analyse and discuss how and if the extra soft ($\Gamma > 5$) steep-decay emission of GRB 090111 fits into different theoretical models; particular attention will be devoted to the possible link with the detected soft prompt 15–150 keV emission. After the steep decay, the GRB 090111 0.3–10 keV light curve shows a peculiar rebrightening, with extreme properties when compared to typical X-ray flares: alternative explanations are discussed. This paper is organized as follows: observations are described in Section 2; the details of the data analysis are reported in Section 3. Our results are discussed in Section 4. Conclusions are drawn in Section 5.

⋆E-mail: raffaella.margutti@brera.inaf.it

Uncertainties and upper limits are quoted at the 90 per cent confidence level (c.l.) unless otherwise stated.

2 *SWIFT* OBSERVATIONS

The *Swift* Burst Alert Telescope (BAT; Barthelmy et al. 2005) triggered and located GRB 090111 at 23:58:21 UT on 2009 January 11. The spacecraft immediately slewed to the burst allowing the X-ray Telescope (XRT; Burrows et al. 2005) and the UV/Optical Telescope (UVOT; Roming et al. 2005) to collect data starting 76.6 and 86 s after the trigger, respectively. A refined position was quickly available: RA(J2000) = $16^{h}46^{m}42\overset{s}{.}14$, Dec.(J2000) = $+00^{\circ}04'38\overset{''}{.}2$ with a 90 per cent error radius of 1.7 arcsec (Evans et al. 2009b). No source was detected by the UVOT at the X-ray afterglow position (Hoversten & Sakamoto 2009). No prompt ground-based observation was reported, probably due to the vicinity (46°) to the Sun.

The data were processed with the HEASOFT v. 6.6.1 package and corresponding calibration files: standard filtering and screening criteria were applied. The BAT data analysis was based on the event data recorded from −240 to 960 s. XRT data were acquired in windowed timing mode until around 150 s; after that time, the XRT automatically switched to the photon counting (PC) mode to follow the decaying source photon flux. Between ∼150 and ∼690 s, PC data were affected by pileup: in this time interval, an annular region of event extraction with the exclusion radius estimated following the prescriptions of Moretti et al. (2005) was used instead of a circular region. The resulting 0.3–10 keV light curve is shown in Fig. 2: the chosen data binning assures a minimum signal-to-noise ratio (SNR) equal to four; when single orbit data were not able to fulfil this requirement, data coming from different orbits were merged to build a unique data point.

3 ANALYSIS AND RESULTS

The BAT light curve (Fig. 1) shows a double-peaked structure with $T_{90}(15\text{–}350\,\mathrm{keV}) = 24.8 \pm 2.7$ s (Stamatikos et al. 2009). It can be fit using two Norris et al. (2005) profiles peaking at $t_{\mathrm{peak},1} = 4.2 \pm 1.2$ s and $t_{\mathrm{peak},2} = 9.3 \pm 1.1$ s; the two structures are characterized by a $1/e$ rise and decay times $t_{\mathrm{rise},1} = 2.6 \pm 0.5$ s, $t_{\mathrm{decay},1} = 6.6 \pm 0.5$ s, $t_{\mathrm{rise},2} = 4.5 \pm 0.4$ s, $t_{\mathrm{decay},2} = 8.8 \pm 1.3$ s and a width $w_1 = 9.1 \pm 1.0$ s and $w_2 = 13.3 \pm 1.6$ s. The amplitude is $A_1 = 0.46 \pm 0.13$ (count s^{-1} cm^{-2}) and $A_2 = 0.38 \pm 0.04$ (count s^{-1} cm^{-2}). The parameters are defined following Norris et al. (2005), while their uncertainty is computed accounting for their covariance and quoted at 68 per cent c.l.

The time-averaged BAT spectrum can be fit by a soft single power-law photon index $\Gamma = 2.37 \pm 0.18$ with a total fluence $S(15\text{–}150\,\mathrm{keV}) = (6.2 \pm 1.1) \times 10^{-7}$ erg cm^{-2} (χ^2/d.o.f. = 55.92/56). The fluence ratio $S(25\text{–}50\,\mathrm{keV})/S(50\text{–}100\,\mathrm{keV}) = 1.29 \pm 0.20$ (68 per cent c.l.) places GRB 090111 at the boundary between X-Ray Rich (XRR) and X-Ray Flash (XRF) events according to the classification of Sakamoto et al. (2008). The BAT data alone are not able to constrain the E_{p} parameter (peak energy of the νF_ν spectrum); however, fixing the low-energy photon index α_{B} of a band model at −1 (typical value for both GRBs and XRFs, see e.g. Sakamoto et al. 2005), we derive $E_{\mathrm{p}} < 32$ keV. Using the E_{p}–Γ relation developed by Sakamoto et al. (2009), we have $E_{\mathrm{p}} < 27$ keV, in agreement with the previous result.

The X-ray light curve (Fig. 2) exhibits a steep decay which is best fit by an SPL with index $\alpha_1 = 5.1 \pm 0.2$ ($\alpha_1 = 4.6 \pm 0.2$) and $T_0 = 0$ s ($T_0 = 9.3$ s, peak time of the second prompt pulse). This is followed by a rebrightening which dominates the light curve

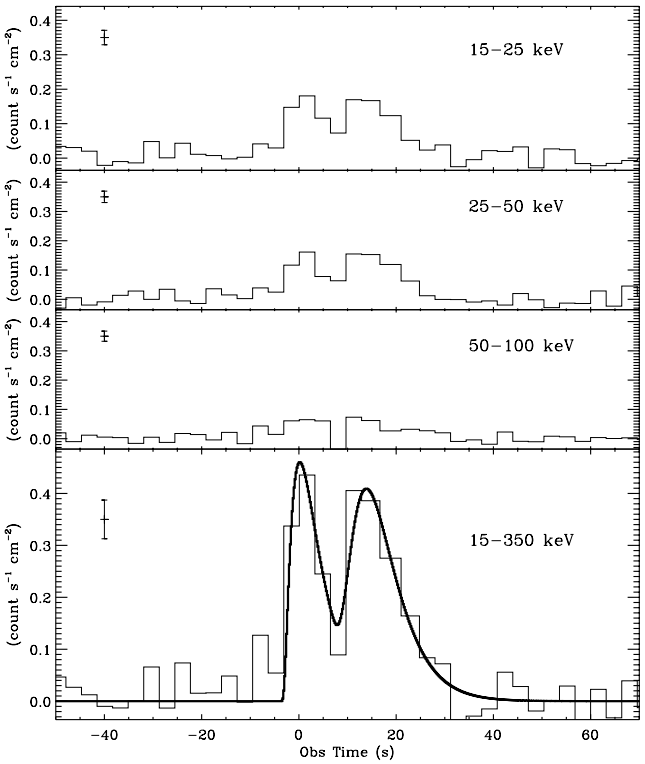

Figure 1. BAT mask-weighted light curve in different energy bands (binning time of 3.2 s). No signal is detected above 100 keV. Bottom panel, solid black line: 15–350 keV light-curve best fit. The typical 1σ error size is also shown in each panel.

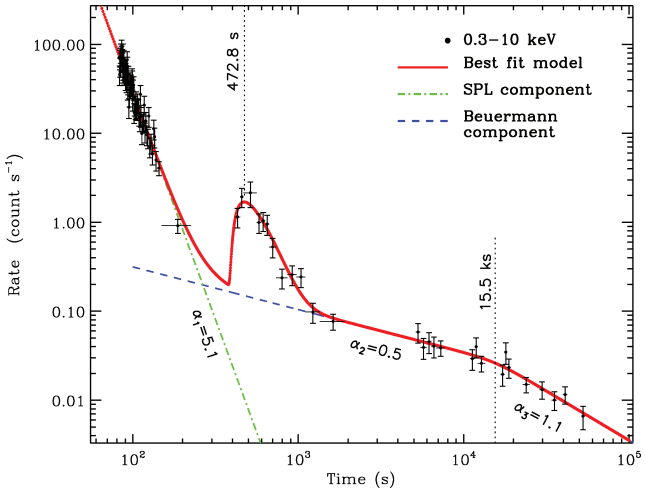

Figure 2. XRT 0.3–10 keV light curve.

between 420 and 900 s. During this time period, no detection can be reported in the 15–150 keV energy range. After the rebrightening, the light curve flattens to an SPL index $\alpha_2 = 0.5 \pm 0.2$, while starting from 15 ks the count rate decays as $\alpha_3 = 1.1 \pm 0.3$ (Fig. 2). The rebrightening can be fit adding a Norris et al. (2005) component with amplitude $A = 1.53 \pm 0.23$ count s^{-1}, start time $t_{\mathrm{s}} = 370$ s (χ^2/d.o.f. = 84.8/93), and rise and decay times $t_{\mathrm{rise}} = 69.3 \pm 8.9$ s and $t_{\mathrm{decay}} = 212.3 \pm 37.5$ s; a width $w = 281.6 \pm 39.2$ s; a peak time $t_{\mathrm{peak}} = 472.8 \pm 21.0$ and an asymmetry parameter $k = 0.51 \pm 0.04$ of Norris et al. (2005). This implies a T_{90} of ∼675 s. In this time interval, the light curve experiences a rebrightening to underlying

continuum fluence ratio $S_{\rm reb}/S_{\rm cont} \sim 4.7$, while the relative flux variability is $\Delta F/F = 14.2 \pm 2.1$ (where ΔF is the rebrightening contribution to the total flux at $t_{\rm peak}$ and F is underlying power-law flux at the same time). All uncertainties related to the light-curve fitting are quoted at 68 per cent c.l.

The steep-decay spectrum ($77 < t < 150$ s) can be modelled using an absorbed SPL with photon index $\Gamma = 5.1 \pm 0.4$ and neutral hydrogen column density $N_{\rm H,0} = (4.9 \pm 0.8) \times 10^{21}$ cm^{-2} in excess of the Galactic value in this direction which is 6.5×10^{20} cm^{-2} (Kalberla et al. 2005) (χ^2/d.o.f. = 68.77/49). While a pure blackbody emission model is ruled out, the addition of a blackbody component statistically improves the fit; however, the data are not able to simultaneously constrain the blackbody temperature and intrinsic absorption so that only rough 2σ limits can be quoted: $0.2 < kT_{\rm b} < 0.8$ keV, $(0.5 < N_{{\rm H},z} < 5) \times 10^{22}$ cm^{-2}. The X-ray data can alternatively be fit by simultaneously modelling the Galactic and host absorption at the proper redshift. We find two sets of allowed parameters: the first is for a close GRB with $N_{{\rm H},z} = (0.63^{+0.14}_{-0.09}) \times 10^{22}$ cm^{-2}, $z = 0.5^{+0.2}_{-0.3}$ and $\Gamma = 4.4 \pm 0.2$ (χ^2/d.o.f. = 40.5/49). The second solution is for a distant and heavily absorbed GRB: $N_{{\rm H},z} = (8.8^{+2.8}_{-6.1}) \times 10^{22}$ cm^{-2}, $z = 3.8^{+0.2}_{-0.3}$ and $\Gamma = 4.0 \pm 0.2$ (χ^2/d.o.f. = 48.6/49). The fit is not able to constrain the redshift parameter; however, the detection of $N_{{\rm H},z}$ in excess of the Galactic value (at $z = 0$) suggests $z < 1.8$ according to the Grupe et al. (2007) relation.

Spectral evolution is apparent from Fig. 3, with the (1 – 2) keV/(0.3 – 1) keV hardness ratio (HR) starting to decrease 100 s after the trigger: it is interesting to note that this corresponds to the end of a period of higher temporal variability detected in the 1–2 keV light curve. This kind of variability is not seen in the 0.3–1 keV data. A comparison of the light curves extracted in the two energy bands reveals a depletion of high-energy photons with time: while the 0.3–1 keV best-fitting SPL decay index is $\alpha_1 = 4.3 \pm 0.3$, the continuum higher energy (1–2 keV) photon flux decay is steeper, being modelled by $\alpha_2 = 5.6 \pm 0.5$.

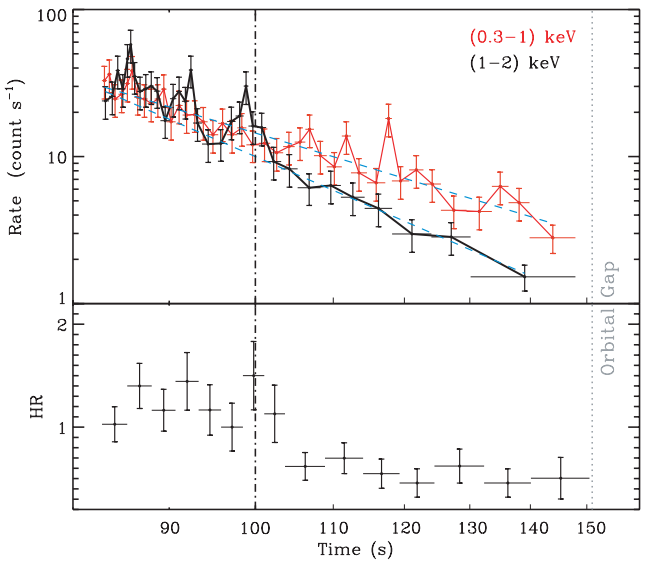

Figure 3. Upper panel: red (black) points: 0.3–1 keV (1–2 keV) XRT light curve rebinned at constant signal-to-noise ratio, SNR = 4. Blue dashed lines: best-fitting SPL models. Lower panel: hardness ratio HR = (1–10) keV/(0.3 – 1) keV evolution with time. The dash–dotted vertical line marks the beginning of the HR decrease.

4 DISCUSSION

4.1 Unusual spectral properties

GRB 090111 shows a very steep ($\alpha = 5.1 \pm 0.2$, 68 per cent c.l.) and soft decay (spectral index $\beta = 4.1 \pm 0.4$): out of 295 GRB X-ray light curves showing the canonical steep–shallow–normal decay transition analysed by Evans et al. (2009a), only 11 (4 per cent) events are characterized by an initial power-law index steeper than the one observed in GRB 090111. Such a high value suggests that this is the beginning of the tail of a flare whose onset was missed by the XRT. The spectral analysis leads to the same conclusion: out of 1242 time-resolved XRT spectra of *Swift* GRB in the time period 2005 April–2008 September , we found the existence of very soft absorbed SPL photon indices $\Gamma > 5$ in GRB050714B, GRB050822 and GRB060512: in each of these cases, the soft spectral emission is linked to flare activity in the XRT light curve. (The three bursts also show a soft BAT prompt emission, with a time-averaged 15–150 keV photon index $\Gamma \sim 2.4$–2.5). If this is the case, the comoving spectrum is likely to be a band spectrum whose $E_{\rm peak}$ evolves to lower values.

Both the BAT prompt photon index steeper than 2 and the XRT photon index $\Gamma > 4$ steeper than the typical band low-energy photon index $\alpha_{\rm B} \sim -1$ (see e.g. Sakamoto et al. 2005; Kaneko et al. 2006) suggest that in both cases the observed emission is dominated by the β portion of the comoving band spectrum. It is interesting to note that fixing $\alpha_{\rm B} \sim -1$ in the prompt spectrum we obtain $28 < E_{\rm peak} < 30$ keV at 3σ level for a high-energy photon index $-5 < \beta_{\rm B} < -4$ which matches the unusual value of the high-energy photons index measured in the XRT. This establishes a spectral connection between the XRT steep decay and the prompt emission, provided that the $E_{\rm peak}$ had shifted well inside the XRT energy range by the beginning of the observation as found in other GRBs and XRFs (e.g. GRB060614, Mangano et al. 2007a; XRF 050416A, Mangano et al. 2007b). At the same time, the very soft emission observed extends the distribution in $\beta_{\rm B}$ to very low values: only ~10 per cent of the spectra of 156 BATSE GRBs either have $\beta_{\rm B} < -4$ or do not have any high-energy component (see e.g. Kaneko et al. 2006).

During the steep decay, spectral evolution is apparent (Fig. 3, lower panel). We split the steep- decay phase into two time intervals, taking 100 s as dividing line as suggested by the HR evolution. A simultaneous fit of the two spectra with an absorbed cut-off power-law model (with $E_{\rm peak}$ as a free parameter of the fit) shows that for each ($N_{{\rm H},z}$, z) couple there exists a statistically acceptable solution with $E_{\rm peak,1} = 1.0^{+0.2}_{-0.1}$ keV and $E_{\rm peak,2} < 0.3$ keV, where the subscripts 1 and 2 refer to the first ($t < 100$ s) and second ($t > 100$ s) time intervals, respectively. This suggests that the detected spectral evolution can be linked to the evolution of the $E_{\rm peak}$ to lower values. It is worth noting that the higher temporal variability characterizing the 1–2 keV signal in the first 100 s (Fig. 3) disappears as the peak energy evolves outside the energy band.

4.2 Peculiar rebrightening: a flare?

Interpreting the X-ray rebrightening as the onset of the afterglow, it is possible to infer the initial Lorentz factor Γ_0 of the fireball from the light-curve peak time (see Molinari et al. 2007 and references therein). For a homogeneous surrounding medium with particle density $n_0 = 1$ cm^{-3}, radiative efficiency $\eta = 0.2$, we have $\Gamma_0 \sim 180(1+z)^{3/8}\ (E_\gamma/10^{53}\ {\rm erg})^{1/8}$. From $z < 1.8$, we derive an intrinsic peak energy $E_{\rm p,i} < 84$ keV and isotropic energy $E_{\rm iso} < 9 \times 10^{51}$ erg (well within the 2σ region of the Amati 2006 relation). This translates

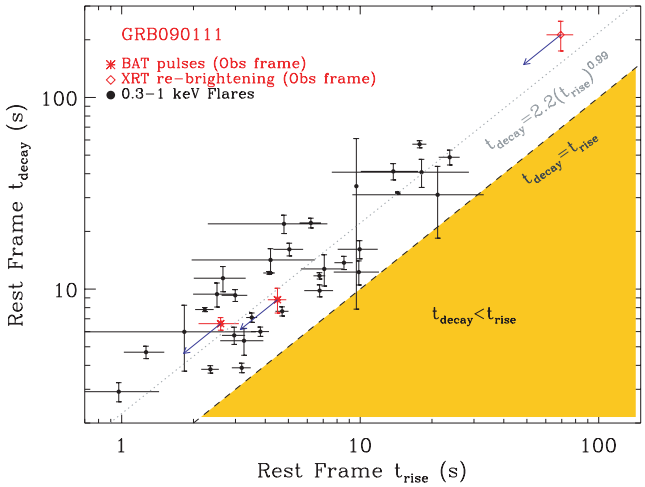

Figure 4. Decay time versus rise time for a subsample of 32 early-time flares identified in the 0.3–10 keV energy range in GRBs with redshift (Chincarini et al., in preparation) and for GRB090111. The blue arrows track the shift of the data when the redshift correction is applied. The black dashed line corresponds to the $t_{\rm decay} = t_{\rm rise}$ locus, while the best-fitting power-law model is indicated with a grey dotted line: $t_{\rm decay} = (2.2 \pm 0.1) t_{\rm rise}^{(0.99\pm0.02)}$ (1σ c.l.).

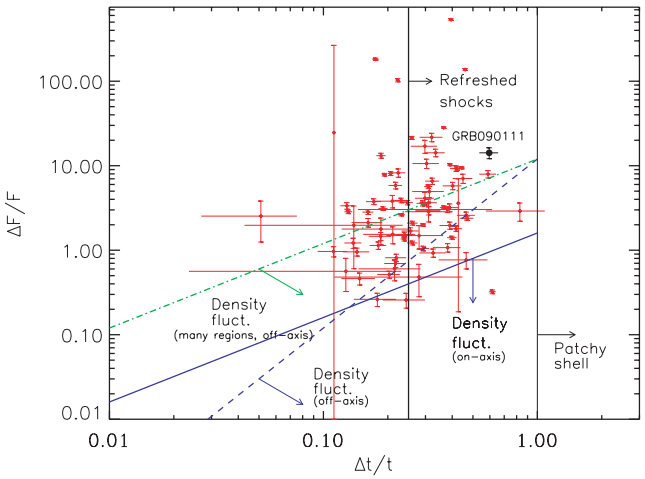

Figure 5. Relative variability flux ($\Delta F/F$) kinematically allowed regions as a function of relative variability time-scale $\Delta t/t$ for a sample of 81 early ($t_{\rm peak,obs} < 1000$ s) flares identified in 54 different GRBs (Chincarini et al., in preparation). The three limits shown have been computed according to equation (7) and (A2) of Ioka et al. 2005. The position of GRB 090111 is marked with a filled black dot.

into a conservative upper limit $\Gamma_0 < 100$: this is lower than what is commonly found for normal GRBs ($\Gamma_0 \sim 500$; see e.g. Molinari et al. 2007), and consistent with the less Lorentz-boosted interpretation of XRRs and XRFs (see Zhang 2007 for a review). A similar result has been found for other XRFs: see, for example, XRF080330 (Guidorzi et al. 2009).

In the context of off-axis emission, it is worth noting that the X-ray rebrightening experienced by GRB 090111 is a sharp feature, reaching a flux contrast $\Delta F/F \sim 14$ during a rising time of only ~70 s. Granot (2005) showed that both on- and off-axis decelerating jets can only produce smooth bumps in the afterglow emission. We therefore consider this hypothesis unlikely.

A much more likely explanation is suggested by Fig. 4 where the temporal properties of the GRB 090111 BAT pulses and of the XRT rebrightening are shown to be consistent with the best-fitting relation found for the intrinsic properties of 32 0.3–10 keV early-time flares (Chincarini et al., in preparation). This fact, together with the consistency with the typical $t_{\rm rise}/t_{\rm decay} \sim 0.3$–$0.5$ (Norris et al. 1996) found for prompt pulses, would suggest a common internal shock origin.

Alternatively, the bump could be due to refreshed shocks (Rees & Meszaros 1998). Following the calculations of Ioka, Kobayashi & Zhang (2005), we plot in Fig. 5 the $\Delta F/F$ and $\Delta t/t$ values for the X-ray bump of GRB 090111 together with the values coming from a homogeneous analysis of 82 early ($t_{\rm peak} < 1000$ s) flares identified in 54 different GRBs by Chincarini et al., in preparation: all the flares (including the GRB 090111 bump) were fit using the same Norris et al. (2005) profile, defining the width of each pulse as the time interval between the $1/e$ intensity points. Fig. 5 shows the kinematically allowed regions for bumps produced by density fluctuations (Wang & Loeb 2000; Dai & Lu 2002; Lazzati et al. 2002) seen on-axis, off-axis and by many regions according to equation (7) and (A2) in Ioka et al. (2005); bumps due to patchy shells (Meszaros, Rees & Wijers 1998; Kumar & Piran 2000) occupy the $\Delta t > t$ region, while refreshed shocks account for the $\Delta t > t/4$ area. From this figure, it is apparent that the X-ray bump of GRB 090111 lies in the refreshed shocks region: density fluctuations are ruled out.

5 CONCLUSIONS

GRB 090111 shows an extra soft $\Gamma > 5$ steep-decay emission. This is likely due to an intrinsic band spectrum whose low-energy power law is missed because of the limited energy range of the XRT. The peak energy of the spectrum evolves through the XRT band producing a softening trend testified by the different light-curve decay behaviours in different energy bands. It is interesting to note that the period of higher temporal variability in the 1–2 keV light curve ends when the $E_{\rm peak}$ shifts outside the energy band. The steep decay is followed by an X-ray rebrightening whose peculiar temporal properties made it worth a detailed study. While the temporal properties of the rebrightening are consistent with an internal origin, with $\Delta t/t \sim 0.6$ and $\Delta F/F \sim 14$, the bump lies in the refreshed shocks region of Fig. 5. Density fluctuations are ruled out. Finally, with a fluence ratio $S(25\text{–}50\,{\rm keV})/S(50\text{–}100\,{\rm keV}) = 1.29 \pm 0.20$ (68 per cent c.l.), we propose this event to be classified as XRR 090111.

ACKNOWLEDGMENTS

This work is supported by ASI grant SWIFT I/011/07/0, the Ministry of University and Research of Italy (PRIN MIUR 2007TNYZXL), MAE and the University of Milano Bicocca (Italy).

REFERENCES

Amati L., 2006, MNRAS, 372, 233
Band D. et al., 1993, ApJ, 413, 281
Barthelmy S. D. et al., 2005, Space Sci. Rev., 120, 143
Burrows D. N. et al., 2005, Space Sci. Rev., 120, 165
Chincarini G. et al., 2007, ApJ, 671, 1903
Dai Z. G., Lu T., 2002, ApJ, 565, L87
Evans P. A. et al., 2009a, MNRAS, 397, 1177
Evans P. A., Goad M. R., Osborne J. P., Beardmore A. P., 2009b, GCN Circ. 8796
Falcone A. D. et al., 2007, ApJ, 671, 1921
Fenimore E. E., Madras C. D., Nayakshin S., 1996, ApJ, 473, 998

Gehrels N. et al., 2004, ApJ, 611, 1005
Granot J., 2005, ApJ, 631, 1022
Grupe D. et al., 2007, AJ, 133, 2216
Guidorzi C. et al., 2009, A&A, 499, 439
Hoversten E. A., Sakamoto T., 2009, GCN Circ. 8799
Ioka K., Kobayashi S., Zhang B., 2005, ApJ, 631, 429
Kalberla P. M. W., Burton W. B., Hartmann D., Arnal E. M., Bajaja E., Morras R., Pöppel W. G. L., 2005, A&A, 440, 775
Kaneko Y., Preece R. D., Briggs M. S., Paciesas W. S., Meegan C. A., Band D. L., 2006, ApJS, 166, 298
Kumar P., Panaitescu A., 2000, ApJ, 541, L51
Kumar P., Piran T., 2000, ApJ, 535, 152
Lazzati D., Rossi E., Covino S., Ghisselini G., Malesani D., 2002, A&A, 396, L5
Mangano V. et al., 2007a, A&A, 470, 105
Mangano V. et al., 2007b, ApJ, 654, 403
Meszaros P., Rees M. J., Wijers R. A. M. J., 1998, ApJ, 499, 301
Molinari E. et al., 2007, A&A, 469, 13
Moretti A. et al., 2005, SPIE, 5898, 360
Norris J. P., Nemiroff R. J., Bonnell J. T., Scargle J. D., Kouveliotou C., Paciesas W. S., Meegan C. A., Fishman G. J., 1996, ApJ, 459, 393
Norris J. P., Bonnell J. T., Kazanas D., Scargle J. D., Hakkila J., Giblin T. W., 2005, ApJ, 627, 324
Nousek J. A. et al., 2006, ApJ, 642, 389
Qin Y.-P. et al., 2009, ApJ, 691, 811
Rees M. J., Meszaros P., 1998, ApJ, 496, L1
Roming P. W. A. et al., 2005, Space Sci. Rev., 120, 95
Sakamoto T. et al., 2005, ApJ, 629, 311
Sakamoto T. et al., 2008, ApJ, 679, 570
Sakamoto T. et al., 2009, ApJ, 693, 922
Stamatikos M. et al., 2009, GCN Circ. 8800
Tagliaferri G. et al., 2005, Nat, 436, 985
Wang X., Loeb A., 2000, ApJ, 535, 788
Zhang B., 2007, Chin. J. Astron. Astrophys., 7, 1
Zhang B. B. Liang E. W., Zhang B., 2007, ApJ, 666, 1002
Zhang B.-B., Zhang B., Liang E.-W., Wang X.-Y., 2009, ApJ, 690, L10

This paper has been typeset from a TEX/LATEX file prepared by the author.